AD_____

Award Number: DAMD17-01-1-0064

TITLE: Endourethral MRI Guidance for Prostatic RF Ablation

PRINCIPAL INVESTIGATOR: Ergin Atalar, Ph.D.

CONTRACTING ORGANIZATION: Johns Hopkins University
School of Medicine
Baltimore, Maryland 21205

REPORT DATE: June 2002

TYPE OF REPORT: Annual

PREPARED FOR: U.S. Army Medical Research and Materiel Command
Fort Detrick, Maryland 21702-5012

DISTRIBUTION STATEMENT: Approved for Public Release;
Distribution Unlimited

The views, opinions and/or findings contained in this report are those of the author(s) and should not be construed as an official Department of the Army position, policy or decision unless so designated by other documentation.

REPORT DOCUMENTATION PAGE

Form Approved
OMB No. 074-0188

Public reporting burden for this collection of information is estimated to average 1 hour per response, including the time for reviewing instructions, searching existing data sources, gathering and maintaining the data needed, and completing and reviewing this collection of information. Send comments regarding this burden estimate or any other aspect of this collection of information, including suggestions for reducing this burden to Washington Headquarters Services, Directorate for Information Operations and Reports, 1215 Jefferson Davis Highway, Suite 1204, Arlington, VA 22202-4302, and to the Office of Management and Budget, Paperwork Reduction Project (0704-0188), Washington, DC 20503

1. AGENCY USE ONLY (Leave blank)	2. REPORT DATE	3. REPORT TYPE AND DATES COVERED
	June 2002	Annual (1 Jun 01 - 31 May 02)

4. TITLE AND SUBTITLE
Endourethral MRI Guidance for Prostatic RF Ablation

5. FUNDING NUMBERS
DAMD17-01-1-0064

6. AUTHOR(S)
Ergin Atalar, Ph.D.

7. PERFORMING ORGANIZATION NAME(S) AND ADDRESS(ES)
Johns Hopkins University School of Medicine
Baltimore, Maryland 21205

E-Mail: eatalar@mri.jhu.edu

8. PERFORMING ORGANIZATION REPORT NUMBER

9. SPONSORING / MONITORING AGENCY NAME(S) AND ADDRESS(ES)
U.S. Army Medical Research and Materiel Command
Fort Detrick, Maryland 21702-5012

10. SPONSORING / MONITORING AGENCY REPORT NUMBER

11. SUPPLEMENTARY NOTES
Report contains color.

20021113 024

12a. DISTRIBUTION / AVAILABILITY STATEMENT
Approved for Public Release; Distribution Unlimited.

12b. DISTRIBUTION CODE

13. ABSTRACT *(Maximum 200 Words)*

MR imaging of the prostate can be greatly improved by using a phased array that combines the signals from individual receiver coils to form a composite image. Endourethral coils and a dual-coil endorectal probe were constructed and combined with a surface coil in a phased array system. Various phased array configurations were tested with *in vivo* canine experiments, which resulted in high-resolution images that clearly showed the anatomy of the prostate and surrounding structures such as the neurovascular bundles. The endourethral coils were useful in imaging the anterior portion of the prostate, while the endorectal coils provided high SNR in the posterior region of the prostate.

14. SUBJECT TERMS
Prostate cancer - Prostate, MRI, phased array, endorectal coil, endourethral coil

15. NUMBER OF PAGES
11

16. PRICE CODE

17. SECURITY CLASSIFICATION OF REPORT	18. SECURITY CLASSIFICATION OF THIS PAGE	19. SECURITY CLASSIFICATION OF ABSTRACT	20. LIMITATION OF ABSTRACT
Unclassified	Unclassified	Unclassified	Unlimited

Table of Contents

A. Introduction

The specific aims of the project were stated as follows in the original application:

We believe that the success of MR-guided therapy of the prostate depends on the improvement in signal-to-noise ratio. Currently, open MR magnets are used for MR-guided thermal therapy. Unfortunately, studies carried out in open magnets suffer from low SNR because of (a) low main magnetic field (it is known that field strength and SNR have a linear relation) and (b) the coils designed for the open magnets are not optimal because scanner manufacturers do not put enough effort into their development. We, therefore, plan to investigate the use of optimum RF coils in high-field short magnets for real-time monitoring of the RF ablation process. More specifically:

Aim 1. We will develop novel MRI probes for acquisition of ultra-high resolution images of the prostate.

Aim 1a. Based on the single-loop technology developed in our lab, we will design tiny and flexible endo-urethral probes with mechanical properties similar to Foley catheters. To obtain maximum performance, we will combine these probes with a homemade endo-rectal MRI probe and two homemade pelvic coils in a phased array combination.

Aim 1b. We will measure the performance of this design on a phantom and compare the results with the ultimate intrinsic SNR.

Aim 1c. We will test the performance and safety of the phased array coil for high-resolution imaging of the prostate on a dog model.

Aim 2. We will test the hypothesis that RF therapy of the prostate can be monitored using real-time MRI techniques on a dog model. For this purpose:

Aim 2a. We will construct an MR-compatible RFT needle in the form of an MRI antenna and connect it to the phased array coil developed in the previous aim to visualize the position of the needle and surrounding tissue during the ablation procedure.

Aim 2b. We will test the hypothesis that RF ablation of the prostate can be monitored in vivo on a dog model.

Aim 3. We will test the hypothesis that MR-guided RF ablation procedures can be carried out without a significant risk of morbidity and mortality on dogs. We plan to use histology as the gold standard for comparison, from which we will derive an effectiveness versus morbidity curve that could be used by clinicians to help determine the extent of ablation therapy.

Our overall aim is to develop an MR-guided prostate therapy system. After successful completion of this project, we will seek further funding to investigate the use of the developed system on human patients.

According the original timeline, part of the Aim 1 would be worked on in the first year and the rest of the aims would be started in the second year. As was proposed, we worked on the first aim in the first year. The design of the coil and its testing is close to completion. Results from this part of the study were presented at the ISMRM and IEEE EMBS meetings.

B. Body

B.1. *Coil design*

In this study, we designed a prostate phased array system that consisted of one 3-inch surface coil (General Electric), one endourethral coil, and two endorectal coils. Two types of endourethral coils were investigated: a loopless design that fit into a 2.5 mm diameter sheath; and a loop design that fit into a 5.3 mm diameter sheath. Two 1.3 x 2 cm rectal loop coils were mounted on the same probe, with the amount of overlap set so that interloop flux was minimized to ensure isolation. All coils were matched and decoupled by the appropriate circuitry.

B.2. *Experimental Methods*

The prostate phased array was compared to a cardiac phased array on a cylindrical polyacrylamide phantom (19 cm diameter, ~ 0.6 S/m). The coils were situated to mimic the coil placement found in a previous *in vivo* canine study, with the prostate considered to be in the center of the phantom (a roughly elliptical region of 4.7 x 4.4 cm in the axial plane). Axial images were obtained using a spin echo sequence that minimized T1 and T2 effects (TE/TR = 9/6000 ms, 256x128, 1 NEX, FOV 22 cm, slice thickness 1.5 mm). SNR for each receiver in the phased array was determined by dividing the signal regions by the standard deviation of noise, which was calculated as the RMS value of all pixel intensities in a selected background ROI, divided by 1.41. The SNR of the combined image is the square root of the sum-of-squares of the individual receiver SNRs.

The amount of isolation between the elements of the prostate phased array was tested in the polyacrylamide phantom using a network analyzer. A series of dog experiments (n=4) was performed. An anesthetized dog was placed supine onto the scanner bed of a 1.5 T GE Signa scanner. Large FOV scout images were acquired to help guide coil placement for maximum coverage of the prostate. The loopless endourethral coil was inserted through the penis to access the prostatic urethra. The prostate was imaged with the phased array using T1- and T2-weighted fast spin echo scans. The loop endourethral probe was surgically placed in the urethra of another dog, (n=1) and imaged separately.

B.3. *Results*

Within the region representing the prostate (i.e., the dashed outline in Figure 1), the prostate phased array performed 2 to 20 times better than the cardiac phased array. The isolation between phased array elements ranged from 18dB (between the two rectal coils) to 22 dB (between the loopless endourethral coil and the surface coil). The unloaded and loaded Q of both rectal coils was 35 and 30, respectively, while the surface coil had an unloaded and loaded Q of 61 and 20.

With this phased array coil, we achieved a resolution of 160 microns.

B.4. *Discussion*

The cardiac phased array is a typical surface coil arrangement that is optimized to image regions deep within the human torso. Phantom experiments showed that the prostate phased array performed significantly better than the cardiac surface phased array where rectal coils were the dominant sources of SNR performance. The loop endourethral coil provides a more significant SNR

contribution than the loopless design used in the current phased array. This loop design has previously been used to image the human female urethra. We anticipate that replacement of the loopless endourethral coil with a loop design will improve the prostate phased array, especially in its sensitivity in the anterior prostate region. The relative contribution of each coil depends on the size of the prostate and its position relative to the coils. The dominance of the rectal coils in this study was partly due to their close proximity to the prostate (-0.8 cm separation). However, if the prostate is larger or farther away from the rectal wall (e.g., in elderly men), the endourethral and surface coils can contribute more significantly to the overall performance. It may be desirable to flatten out the uneven intensity variation due to the phased array. If the location and orientation of each coil is known, the raw image data can be re-normalized on the basis of *a priori* knowledge of each coil's field distribution.

C. Key Research Accomplishments

We are close to completion of the specific Aim 1 of the project. This matches the proposed timeline of the project.

D. Reportable Outcomes

We have presented the results of the study at the ISMRM and IEEE EMBS meetings. The journal paper is in preparation. We plan to submit the paper to Magnetic Resonance in Medicine.

E. Conclusions

We completed most of Aim 1 of the study by designing a phased array of endorectal, endourethral, and surface coils that produced images of the canine prostate with a resolution of up to 160 microns. We plan to publish our results in a peer-reviewed journal.

F. References

1. A. C. Yung, Y. A. Oner, J. M. Serfaty, M. Feleney, X. Yang, E. Atalar, Phased Array Coils for High Resolution Prostate MR Imaging, IEEE EMBS, Istanbul, Turkey, 2001.
2. A. .C Yung, A. Y. Oner, J. M. Serfaty, M. Feneley, X. Yang, E. Atalar, High Resolution Imaging of Canine Prostate using Endorectal/Endourethral Phased Array Coils, ISMRM, Book of abstracts Paper#1896, Honolulu, HI, 2002.

High Resolution Imagir f Canine Prostate Using Endorectal/Endor hral Phased Array Coils

A.C. Yung, A.Y. Oner, J.-M. Serfaty, M. Feneley, X. Yang, E. Atalar
Johns Hopkins University, Baltimore, MD, USA

Abstract

A phased array system of one surface, two endorectal, and one loopless endourethral coil was designed to image the canine prostate. A loop endourethral coil was also investigated in a separate study. A phantom study indicated that our phased array system outperforms a cardiac surface coil phased array by a factor of 2 to 20 within the region of interest. For *in vivo* canine experiments, T2-weighted FSE images of the prostate were acquired with pixel sizes of 160 μm. The loop endourethral coil alone generated images with a resolution of 312 μm. We believe that this phased array can be used to increase the sensitivity of MRI in prostate imaging, thus increasing accuracy of cancer staging.

Introduction

Prostate cancer is highly prevalent in elderly men, with 50% of men over the age of 80 diagnosed with some form of the disease [1]. Accurate staging of the cancer is necessary to select the best treatment option. Transrectal ultrasound (TRUS) is the most common imaging modality used in staging the cancer; however, it has been reported that only 60% of tumors are visible with TRUS [2]. MRI, with its excellent soft tissue contrast, has been investigated as an alternative technique. It has been shown that the ability of MRI to determine staging is improved when an endorectal coil is combined with a surface coil in a phased array configuration [2]. This work attempts to extend the state-of-the-art in prostate MR imaging by introducing more coils in the phased array, both endorectally and endourethrally. A number of receiver coils were constructed, and *in vivo* canine experiments were conducted to test their performance.

Coil Design

The prostate phased array system consisted of one 3-inch surface coil (General Electric), one endourethral coil, and two endorectal coils. Two types of endourethral coil were investigated: a loopless design fitting in a 2.5 mm diameter sheath [3]; and a loop design in a 5.3 mm diameter sheath [4]. Two 1.3 x 2 cm rectal loop coils were mounted on the same probe, with the amount of overlap set so that interloop flux was minimized to ensure isolation. All coils were matched and decoupled by the appropriate circuitry.

Experimental Methods

The prostate phased array was compared to a cardiac phased array on a cylindrical polyacrylamide phantom (19 cm diameter, σ=0.6 S/m). The coils were situated to mimic the coil placement found in a previous *in vivo* canine study, with the prostate considered to be in the center of the phantom (a roughly elliptical region of 4.7 x 4.4 cm in the axial plane). Axial images were obtained using a spin echo sequence that minimized T1 and T2 effects (TE/TR = 9/6000 ms, 256x128, 1 NEX, FOV 22 cm, slice thickness 1.5 mm). SNR for each receiver in the phased array was determined by dividing the signal regions by the standard deviation of noise, which was calculated as the RMS value of all pixel intensities in a selected background ROI, divided by $\sqrt{2}$ [5]. The SNR of the combined image is the square root of the sum-of-squares of the individual receiver SNRs.

The amount of isolation between the elements of the prostate phased array was tested in the polyacrylamide phantom using a network analyzer.

A series of dog experiments (N=4) was performed. An anesthetized dog was placed supine onto the scanner bed of a 1.5 T GE Signa scanner. Large FOV scout images were acquired to help guide coil placement for maximum coverage of the prostate. The loopless endourethral coil was inserted through the penis to access the prostatic urethra. The prostate was imaged with the phased array using T1- and T2-weighted fast spin echo scans. The loop endourethral probe was surgically placed in the urethra of another dog (N=1) and imaged separately.

Results

Figure 1 shows the prostate phased array SNR divided by the cardiac phased array SNR, as imaged in the polyacrylamide phantom. Within the region representing the prostate (i.e., the dashed outline in Figure 1), the prostate phased array performed 2 to 20 times better than the cardiac phased array.

The isolation between phased array elements ranged from 18 dB (between the two rectal coils) to 22 dB (between the loopless endourethral coil and the surface coil). The unloaded and loaded Q of both rectal coils was 35 and 30, respectively, while the surface coil had an unloaded and loaded Q of 61 and 20.

Figure 2 shows a T2-weighted FSE axial image generated by the endorectal coils, the 3-inch surface coil, and the loopless endourethral coil. A resolution of 160 μm was achieved (TR/TE=3100/72.7 ms, ETL=32, 512x512, NEX=16, FOV 8cm, slice thickness=1.5 mm, scan time=13:20 min). Figure 3 shows a coronal image of another canine prostate, obtained using only the endourethral loop coil. A resolution of 312 μm was achieved (FSE, TR/TE=3500/102 ms, ETL=32, 256 x 256, NEX=8, FOV 8cm, slice thickness= 1.5mm, scan time=3:44 min).

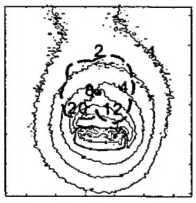

Fig. 1 – SNR ratio of prostate phased array vs. cardiac phased array.

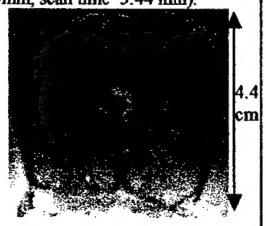

Fig. 2 – T2-weighted axial image of canine prostate (160 μm resolution).

Fig. 3 – Coronal image from loop endourethral coil.

Discussion

The cardiac phased array is a typical surface coil arrangement that is optimized to image regions deep within the human torso. Phantom experiments showed that the prostate phased array performed significantly better than the cardiac surface phased array, where rectal coils were the dominant sources of SNR performance. The image in Figure 3 suggests that the loop endourethral coil may provide a more significant SNR contribution than the loopless design used in the current phased array. This loop design has previously been used to image the human female urethra at a resolution of 94 x 156 μm [4]. We anticipate that replacement of the loopless endourethral coil with a loop design will improve the prostate phased array, especially in its sensitivity in the anterior prostate region.

The relative contribution of each coil depends on the size of the prostate and its position relative to the coils. The dominance of the rectal coils in this study was partly due to their close proximity to the prostate (~0.8 cm separation). However, if the prostate is larger or farther away from the rectal wall (e.g., in elderly men), the endourethral and surface coils can have a more significant contribution to the overall performance.

It may be desirable to flatten out the uneven intensity variation due to the phased array. If the location and orientation of each coil is known, the raw image data can be renormalized on the basis of *a priori* knowledge of each coil's field distribution.

We plan to use the prostate phased array for image guidance of minimally invasive therapies for prostate cancer.

Conclusion

We developed a phased array of endorectal, endourethral, and surface coils that produced images of the canine prostate with a resolution of up to 160 μm. We believe that this phased array configuration can further increase the sensitivity of MRI in detecting and staging prostate cancer.

Acknowledgments

The authors thank Robert Susil for technical advice and Mary McAllister for assistance with manuscript preparation.

References

[1] Parkin DM, et al. *CA Cancer J Clin*, 49:33-64, 1999. [2] Wilkinson BA et al., 87(5):423-430 [3] Yung AC et al.", *Proc. EMBS 2001, #1046.* [4] Quick HH et al., MRM 45:138-146, 2001. [5] Constantinides CD et al., *MRM* 38:852-857, 1997.

PHASED ARRAY COILS FOR HIGH RESOLUTION PROSTATE MR IMAGING

Andrew C. Yung, A. Yusuf Oner, Jean-Michel Serfaty, Mark Feleney, Xiaoming Yang, Ergin Atalar
Johns Hopkins University, Baltimore, Maryland, USA

Abstract – **MR imaging of the prostate can be greatly improved by using a phased array that combines the signals from individual receiver coils to form a composite image. Endourethral coils and a dual-coil endorectal probe were constructed and combined with a surface coil in a phased array system. Various phased array configurations were tested with *in vivo* canine experiments, which resulted in high-resolution images that clearly showed the anatomy of the prostate and surrounding structures such as the neurovascular bundles. The endourethral coils were useful in imaging the anterior portion of the prostate, while the endorectal coils provided high SNR in the posterior region of the prostate.**

Keywords – **prostate, MRI, phased array, endorectal coil, endourethral coil**

I. INTRODUCTION

Prostate cancer is the second leading cause of death in aging American men, with more than 50% of men over 80 years of age diagnosed with some form of the disease [1]. In light of the prevalence of this disease in such a large segment of the population, much work has been done to develop methods to help diagnose and treat prostate cancer. Examples of treatment options include traditional surgical resection, chemotherapy, and minimally invasive techniques, such as cryoablation, thermal ablation, and seed brachytherapy.

Many of these emerging technologies depend on an accurate image of the prostate during diagnosis (especially in needle biopsies), preoperative evaluation, and intraoperative image guidance. MRI has been identified as an ideal imaging modality for these purposes due to its excellent soft tissue contrast and higher resolution, compared to ultrasound and CT. Receiving coils are placed at or near the prostate to achieve higher resolution at smaller FOV; this usually is in the form of an endorectal coil, which is situated in the rectum in close proximity to the posterior floor of the prostate. Examples of endorectal coil use include needle biopsy guidance [2] and image guidance of prostate brachytheraphy in a 0.5 T MRI system [3].

Another way to improve prostate imaging is to combine multiple imaging coils into one phased array system, where the signals from individual antennas are incorporated into one composite image. In this way, the overall field of view is increased, while still preserving the local SNR of each coil element of the array. A few instances of phased array systems for prostate imaging exist in the literature; however, most of these are limited to two elements in the phased array. Examples include a double-coil quadrature surface array in a 3 T system [4], and an endorectal-surface coil system for preoperative evaluation of prostatectomy [5].

Here we attempt to extend the current state of the art in phased array prostate imaging by adding more elements to the array and by using different types of coils as elements. In particular, endourethral coils are employed to image the regions of the prostate surrounding the urethra. Endourethral coils are a relatively new technology never before used in prostate MRI, and are described more fully in the literature [6]. To validate our ideas, custom endorectal and endourethral imaging coils were constructed. Various combinations of endorectal coils, endourethral coils, and surface coils were investigated using the canine prostate as an experimental model.

II. METHODS

Several antennas were constructed for use in prostate imaging. Two types of endourethral coil were implemented (loop and loopless), and a dual-coil endorectal probe was also constructed (Figure 1). To simulate the loaded conditions *in vivo*, the matching, detuning, and Q characteristics of each coil were verified using a network analyzer with the coils immersed in a tub of water (50 x 37 x 20 cm). In addition, several commercially available coils were evaluated for use in the phased array system: this included a standard cardiac surface coil, a pelvic surface coil, and an endorectal probe employing an inflatable balloon for stability (Medrad Inc., Indianola PA). In addition, a 16 Fr loop coil that was originally meant for endourethral use was instead used endorectally in one of the canine prostate studies. Various combinations of up to four imaging coils were connected to the input of a 1.5 T GE Signa scanner, which took the sum of the individual squared magnitudes to produce a composite image.

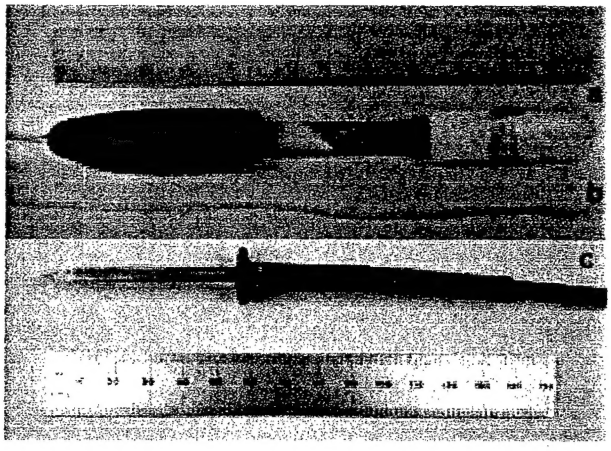

Fig. 1. The (a) dual-coil endorectal probe, (b) loopless endourethral coil, and (c) loop endourethral coil

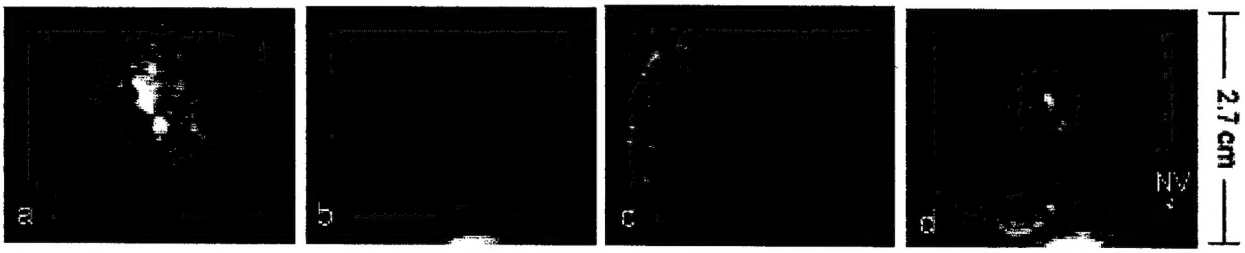

Fig. 2. Axial images of dog prostate for (a) loopless endourethral, (b) 16 Fr. endorectal coil, (c) surface pelvic coil, and (d) combined phased array system. Sequencing parameters: fat-saturated T2-weighted FSE; TR/TE = 4000/100 ms; NEX=8; FOV = 8 x 8 cm; matrix 256 x 256; slice thickness = 3 mm. Legend: NV = neurovascular bundle

A. Endourethral Coil Design

Loopless Design

A loopless coil consists of a coaxial inner conductor extending a quarter-wavelength away from the end of the grounded outer conductor, thus forming a dipole antenna. The loopless coil used in the experiment is encased in a polymeric sheath with an outer diameter of 2.5 mm. A small-diameter coaxial cable is used to convey the antenna's signal to a shielded box containing a matching and detuning circuit.

Matching is achieved by a standard impedance network consisting of nonmagnetic chip capacitors and wirewound inductors. Detuning of the coil during the transmit phase of the body coil is achieved through the use of a PIN diode. During RF transmission, the scanner triggers a DC bias voltage that switches on the PIN diode, which creates a resonant LC tank circuit that presents a very high impedance to the antenna. Thus, the antenna is decoupled until the transmit mode ends and the PIN diode is switched off, thereby preventing the coil from interfering with the excitation's flip angle. A balun was implemented in the matching/detuning box to eliminate shield currents. The balun consists of a coiled coaxial wire and a parallel capacitor connecting the network ground to the scanner ground. This resonant LC tank circuit was designed to "choke" any noise currents from the scanner ground.

Loop Design

The endourethral loop coil used in prostate imaging consists of a copper trace etched as a square loop on a piece of flexible polyimide film. This flexible circuit is ensheathed in polymer tubing that has an outer diameter of 5 mm, and is connected to the scanner inputs via a small-diameter coaxial cable.

Again, chip capacitors are used to match the antenna to the scanner, and a PIN diode is used for decoupling. However, these components are soldered directly onto the flex circuit itself, in order to preserve the antenna's high Q. A "bazooka balun" was constructed from a $\lambda/4$ length of copper braiding, with one end shorted to the coaxial ground.

B. Dual-coil Endorectal Probe Design

The endorectal imaging probe was constructed with two loop coils mounted close together to increase the effective field of view along the basolateral direction of the prostate, while preserving the high SNR of each coil. Each loop coil is exactly analogous in design to the endourethral loop coil described previously. Both loop coils were etched onto standard phenolic PCB board, one on each side and slightly overlapping each other. Each loop is 24 mm x 14 mm and rectangular in shape, while the entire circuit board (6.2 cm x 2.0 cm) is mounted on a tapered silicone probe head attached to a 24 cm plastic handle. The probe head was coated with a protective plastic and covered with a condom.

Reduction of crosstalk between the two loop coils was an important consideration in the probe design. The preferred solution to crosstalk reduction was to determine the optimal amount of overlap between the two coils so that the inward and outward flux exactly cancels. However, since the ideal amount of overlap was unknown prior to the coils being etched, strips of adhesive copper tape (3M) were applied onto one side of the board to block some of the interloop flux, thus decreasing the effective amount of coil overlap. The elimination of crosstalk was verified by ensuring that no artifact was seen when the endorectal coils were imaged in water by the scanner's body coil.

C. In Vivo Studies

The use of phased arrays was investigated with *in vivo* imaging studies of the canine prostate. These experiments were conducted in accordance with all regulations set forth by the relevant institutional and governmental agencies. The dogs were anesthetized prior to the procedure and placed supine on the scanner bed, caudal end first. Large-FOV scout images were acquired to help guide coil placement so that the most sensitive parts of the endourethral and endorectal coils were closest to the prostate. A variety of fast spin echo (FSE), T2-weighted imaging scans were then taken in the region of the prostate. The field of view in each case was kept small (8 cm) with encoding steps of 256 x 256; the resultant pixel size was 0.31 mm.

III. Results

A. In vivo studies

Various combinations of coils were used to implement the phased array system in each experiment. Figure 2 shows axial images produced by a phased array consisting of a loopless endourethral coil, a 16 Fr catheter loop coil in the rectum, and a pelvic surface coil. Figure 3 shows images of the prostate and rectum generated by the phased array consisting of the loopless endourethral coil and the dual-coil endorectal probe. The various layers of the rectal wall can be seen clearly from Figure 3b. It is important to note that Figures 3a and 3b are from the same acquired image but were separated into two images, so that the contrast levels for each could be adjusted separately. Phased arrays with the loop endourethral coil have not yet been implemented; however, a typical image produced by such a coil has been included for comparison (Figure 4). Insertion of this loop coil required surgery, since it was too large to fit through the canine urethra.

B. Coil performance

For the images shown in Figure 2, the matching of the endourethral loopless coil was adequate, with a reflection coefficient ρ of 0.3. Figure 2d shows the phased array's ability to image the neurovascular bundles near the posterior base of the prostate.

Performance of the dual-coil endorectal probe was generally excellent. The magnitude of reflection coefficients for both coils was less than 0.1 under loaded conditions in vivo. Elimination of crosstalk was achieved at the frequency of interest (crosstalk isolation = –30 dB at 63.9 MHz).

IV. Discussion

The images show that the dual-coil endorectal probe and the endourethral coils alone are able to produce high resolution images of the prostate and surrounding structures, with a resolution of at least 0.31 mm. The dual-coil endorectal probe maintained high SNR all along the posterior side of the prostate, and indeed was the dominant source of signal in the image. It was demonstrated that the neurovascular bundles near the base of the prostate can be clearly visualized; it is important to identify these structures to prevent any harm to them during interventions. The phased array system also allows good visualization of the rectal wall, which is helpful in determining the extracapsular spread of the prostate cancer. In turn, it was demonstrated that the loopless endourethral coil provided good coverage of the anterior portion of the prostate.

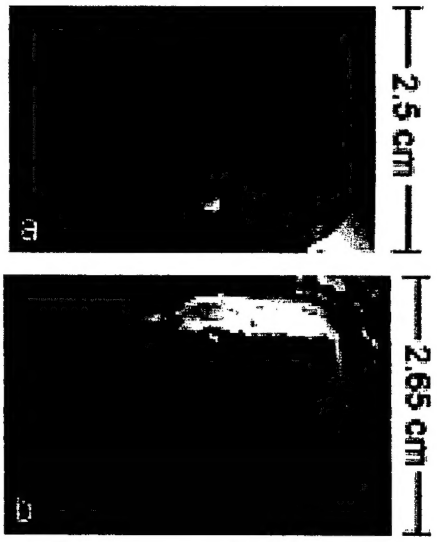

Fig. 3. Phased-array axial image of (a) prostate and (b) rectal wall, obtained by the phased array of the loopless endourethral coil and the dual-coil endorectal probe. The mucosa, submucosa, and muscle layers of the rectal wall can be seen clearly. Sequencing parameters: non-fat-saturated T2-weighted FSE; TR/TE = 4000/160 ms, NEX=8, FOV = 8 x 8 cm, matrix 256 x 256, slice thickness = 2 mm.

It would appear that a phased array of endorectal, endourethral, and surface coils is optimal for prostate imaging; in particular, the endorectal and endourethral coils generate high SNR in distinctly different anatomical regions of the prostate.

Figures 3a and 3b shows a current limitation of the phased array approach to MR imaging: the image had to be separated into two individual images, so that contrast could be adjusted separately to optimize visualization of detail in each region. Each region has a different range of signal intensities, so adjustment of contrast to elucidate features in one region may obscure another part of the image by making the pixels too dark or too bright. However, this limitation can be overcome by appropriate correction algorithms. If the location and orientation of each coil is known, a correction algorithm could renormalize the raw image data on the basis of *a priori* knowledge of each coil's field distribution. Such an algorithm needs to be investigated for use in real-time interventional settings.

One way to improve the phased array is to use a loop design for the endourethral coil rather than a loopless design. The benefit is that the SNR and Q of a loop coil are much higher than is achievable with loopless antennas. However, use of the endourethral loop coil is impractical for a canine model, since the dog urethra is smaller than the loop (at least 15 Fr), which therefore requires difficult surgical transection to achieve placement. Use of such a coil may be more feasible for human studies, where the urethra is much larger.

The endorectal probe can also be improved: a third coil can be added to further increase the effective field of view.

The results gleaned from the canine prostate model, while instructive, do not entirely mimic the situation in the human prostate. The canine prostate has none of the zonal anatomy that the human prostate possesses; distinction of these zones is important because it has been shown that cancer nodes are more likely to form in certain zones than others (the peripheral zone in particular). The dog prostate is typically smaller than the human prostate, especially when compared to the enlarged prostates that are commonly found in aging men. There were also no cancer nodes in the canine prostates that we examined, thus the phased array's ability to differentiate cancerous tissue could not be tested in these experiments. Human studies must be performed to validate the phased array's utility in detecting prostate cancer.

V. Conclusion

Early results suggest that a phased array system of endorectal coils, endourethral coils and surface coils produce high-resolution images of the prostate that are of very high quality. This capability to generate high resolution prostate images will become increasingly important as diagnosis and treatment options for prostate cancer continue to evolve.

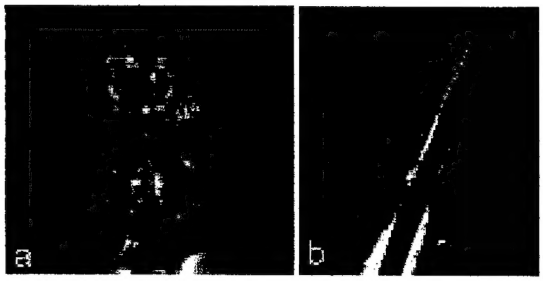

Fig. 4. Comparison of coronal images of dog prostate for (a) loop endourethral coil and (b) loopless endourethral coil.

Acknowledgement

The authors thank Mary McAllister for editorial assistance. The authors are also grateful to Ken Rent for preparation of the animals and Robert C. Susil for technical advice.

References

[1] D. M. Parkin, P. Pisani, and J. Ferlay, "Global cancer statistics," *CA Cancer J Clin*, vol. 49, pp. 33-64, 1., 1999.

[2] R. Watkins, K. Rohling, E. Uzgiris, D. C., D. R., and G. R., "Magnetic Resonance Image Guided Biopsy in Prostate," Proceedings of the ISMRM 2000, p. 412.

[3] J.D. McTavish, R. Cormack, F.A. Jolesz and C.M.C. Tempany., "Evaluation of Interventional MRI (0.5T) of the Prostate Gland Compared to Endorectal Coil MRI (1.5T) in Men Undergoing MR Guided Prostate Brachytherapy," *Proceedings of the ISMRM 1999*, pp. 1972, 1999.

[4] H.-W. Kim, D. L. Buckley, D. Peterson, R. Duensing, P. Narayan, and S. J. Blackband., "Prostate MRI and MRS at 3 Tesla using a Transceive Phased-array Pelvic Coil," Proceedings of the ISMRM 1999, p. 116.

[5] M. Engelbrecht, J. Barentsz, G. Jager, H. V. d. Boogert, and J. D. I. Rosette., "Magnetic Resonance Imaging of Prostate Cancer: Pelvic Phased-Array Coils Versis Integrated Endorectal Pelvic Phased-Array Coils," Proceedings of the ISMRM 1999, p. 1101.

[6] H. H. Quick, J. M. Serfaty, H. K. Pannu, R. Genadry, C. J. Yeung, and E. Atalar, "Endourethral MRI," *Magn Reson Med*, vol. 45, pp. 138-46, 2001.